JCS ePress online publication date 19 April 2005

Manipulation of redox signaling in mammalian cells enabled by controlled photogeneration of reactive oxygen species

Yehudit Posen[1], Vyacheslav Kalchenko[1], Rony Seger[1], Alexander Brandis[2], Avigdor Scherz[2] and Yoram Salomon[1,*]

[1]Department of Biological Regulation, Weizmann Institute of Science, PO Box 26, Rehovot 76100, Israel
[2]Department of Plant Sciences, Weizmann Institute of Science, POB 26, Rehovot 76100, Israel
*Author for correspondence (e-mail: yoram.salomon@weizmann.ac.il)

Accepted 11 February 2005
Journal of Cell Science 118, 1957-1969 Published by The Company of Biologists 2005
doi:10.1242/jcs.02323

Summary

Reactive oxygen species (ROS) comprise a group of noxious byproducts of oxidative processes which participate in the induction of many common diseases. However, understanding their role in the regulation of normal physiological redox signaling is currently evolving. Detailed study of the dynamic functions of ROS within the biological milieu is difficult because of their high chemical reactivity, short lifetime, minute concentrations and cytotoxicity at high concentrations. In this study, we show that increasing intracellular ROS levels, set off by controlled in situ photogeneration of a nontoxic bacteriochlorophyll-based sensitizer initiate responses in cultured melanoma cells. Using hydroethidine as detector, we determined light-dependent generation of superoxide and hydroxyl radicals in cell-free and cell culture models. Monitoring the ROS-induced responses revealed individual and differential behavior of protein kinases [p38, mitogen-activated protein kinase (MAPK), extracellular signal-regulated kinase (ERK), c-Jun N-terminal kinase (JNK) and Akt] as well as effects on the subcellular distribution of phosphorylated p38. Furthermore, alterations in morphology and motility and effects on cell viability as a function of time and photosensitizer doses were observed. Following mild ROS challenge, enzymatic and cellular changes were observed in the majority of the cells, without inducing extensive cell death. However, upon vigorous ROS challenge, a similar profile of the overall responses was observed, terminating in cell death. This study shows that precisely controlled photogeneration of ROS can provide simple, fine-tuned, noninvasive manipulation of ROS-sensitive cellular responses ranging from individual enzymes to gross behavior of target cells. The observations made with this tool enable a dynamic and causal correlation, presenting a new alternative for studying the role of ROS in cellular redox signaling.

Key words: Redox regulation, Signaling, MAPK, ROS, Photodynamic therapy (PDT), Hydroethidine

Introduction

Oxygen's innate oxidizing power forms the basis of toxic oxidative stress via highly reactive oxygen species (ROS) when their levels overwhelm the cellular antioxidant capacity (Halliwell, 1999). However, the classical view of ROS toxicity has been revolutionized as their role in redox regulation of physiological functions is being recognized. The ease with which various ROS cross the cell membrane, their high chemical reactivity and consequential short half-life make them ideal candidates for cellular messengers. Growing evidence indicates that ROS and the ensuing redox state regulate a variety of key cellular functions via direct alterations of enzymes such as protein kinases (Barrett et al., 1999; Gotoh and Cooper, 1998; Lander et al., 1997) or phosphatases (Barrett et al., 1999; Kamata et al., 2000; Lee et al., 1998; Nemani and Lee, 1993; Robinson et al., 1999). Alternatively, ROS can indirectly modulate molecules containing high thiol-disulfide oxidation potentials, such as thioredoxin or glutathione S-transferase (Adler et al., 1999a; Adler et al., 1999b; Saitoh et al., 1998) and thereby influence cellular processes. It has been shown that ROS play a significant role in mediation of inflammatory defense mechanisms (Darrah et al., 2000; Davies, 1995; Vazquez-Torres et al., 2000), regulation of transcription factors (Devary et al., 1991; Meyer et al., 1993), enzyme activity (Lopez-Ongil et al., 2000), cell proliferation (Preston et al., 2001; Kim et al., 2001) and various other crucial physiological signal transduction pathways (Finkel, 2000; Kamata and Hirata, 1999; Remacle et al., 1995; Suzuki et al., 1997). Exogenously applied oxidants, such as H_2O_2, can mimic cellular responses to physiological stimulants, including the stimulation of cell metabolism and growth via the insulin, epidermal growth factor (EGF) or platelet-derived growth factor (PDGF) receptors (Fantus et al., 1989; Gamou and Shimizu, 1995; Hayes and Lockwood, 1987; Heffetz et al., 1990; Knebel et al., 1996). Oxidants have been shown to activate receptor tyrosine kinases (RTKs) and their downstream signaling components including mitogen-activated protein kinases (MAPKs) (Gamou and Shimizu, 1995; Guyton et al., 1996; Kim et al., 2001; Klotz et al., 1999; Knebel et al., 1996). Similarly, oxidative stress has demonstrated effects on protein kinase B (PKB/Akt) in various cellular processes mediated by phosphoinositide 3-kinase (Deora et al., 1998) and heat shock

protein 27 (HSP27) (Konishi et al., 1997; Plaks et al., 2004). However, the specific signaling molecules targeted by physiologically generated or exogenously applied ROS remain ill defined.

The elusive nature of ROS, their profound chemical reactivity and short life span, combined with the complexity of their detection in the physiological milieu retards the study of their role in biology. In an attempt to tightly regulate ROS doses at temporal and spatial, as well as at type-specific levels, we made use of a bacteriochlorophyll-based (Bchl) photosensitizer (Scherz et al., 1997; Scherz et al., 2000; Scherz et al., 2001; Scherz et al., 2003) which allowed for controlled, in situ generation of ROS upon illumination at a wavelength matching its absorption spectrum. This compound and other bacteriochlorophyll-based molecules have been used for generation of cytotoxic levels of ROS in photodynamic therapy (PDT) of different malignancies (Koudinova et al., 2003; Preise et al., 2003; Schreiber et al., 2002; Zilberstein et al., 2001) and for modeling superoxide dismutase activity (Ashur et al., 2003). The ROS profile generated by each sensitizer has been determined using electron spin resonance (ESR)-based analyses, time resolved optical spectroscopy and photochemical products analyses under cell-free conditions (Vakrat et al., 1999; Vakrat-Haglili et al., 2002; Vakrat-Haglili et al., 2005) and have been shown to include O_2^-, $OH^{\cdot}$ and singlet oxygen. The specific ROS generated are highly dependent on the microenvironment in which the photosensitization takes place and are thus expected to induce distinct effects on cellular components situated in each environment. Pd-bacteriochlorophyll derivatives have been shown to largely generate protonated superoxide in lipophilic environments, while generating superoxide and hydroxyl radicals at the lipid/water interface (Vakrat-Haglili et al., 2005). Similarly, because of the innate variance in the half-life of each species (nanoseconds for hydroxyl radical and seconds for superoxide) and the consequential radius of activity (Angstrom and micrometer, respectively), the distance at which the affected molecule is situated will also determine the nature of the response. Furthermore, these photosensitizers can localize extracellularly or intracellularly, depending on their chemical properties, without influencing cell functions in the absence of light (Berg and Moan, 1997). They can also be specifically targeted to certain cell types or subcellular compartments (Akhlynina et al., 1997; Gross et al., 1997) and will generate ROS only upon illumination. Thus, photosensitizers can be employed as a means of manipulating localized ROS production, where fine-tuning of sensitizer concentrations and light intensity and duration can easily regulate the studied biological response. In the context of mild ROS challenge, we refer to the photosensitizer as a photoswitch that can regulate reversible physiological responses without induction of cell death.

The unique chemical nature of ROS singles them out as superb candidates for self-limiting messengers in cell signaling, yet their exact role as generators or mediators of physiological stimuli remains largely unclear. This study considers the role of both mild and vigorous ROS challenge, in cultured cells, by employing Pd-bacteriochlorophyll-serine (Pd-Bchl-Ser) and light as a novel photoswitch for ROS generation, whereby the location and concentration of the photogenerated ROS can be controlled within a physiologically relevant range. Herein, we show generation of superoxide and hydroxyl radicals under cell-free conditions and in cultured cells. While cell death is the hallmark of PDT, the objective of the proposed study is to define the conditions under which such treatment can be used for controlled, mild ROS production, and to analyze the physiological responses of the viable cells to oxidative stress. Our results demonstrate that a given range of Pd-Bchl-Ser concentrations in conjunction with light, can produce low, physiologically relevant ROS concentrations that can trigger responses in live cells in a controlled, time-dependent manner. Such generation of ROS results in selective modifications of specific protein kinases and downstream signaling pathways that lead to cellular responses ranging from changes in cell morphology and motility to cell death.

Materials and Methods

Cell culture

Mouse M2R melanoma cell monolayers were maintained at 37°C in 8% CO_2 as previously described (Gerst et al., 1989). Fetal calf serum was purchased from Biological Industries (Beit Haemek, Israel).

Photosensitizer

O-[Pd-bacteriochlorophyllide]-serine methyl ester (Pd-Bchl-Ser) was prepared as previously described (Brandis et al., 2005). The pigment was dissolved in 95% ethanol and diluted in cell culture medium to a final concentration of 1% ethanol.

Light source

A home built 100 W halogen lamp equipped with a high pass filter (λ>650 nm, Safelight filter 1A; Eastman Kodak Co., Rochester, NY) and a 4 cm water filter were used to illuminate (20 mW/cm^2/10 minutes; 12 J/cm^2) the culture plates from the bottom, at room temperature, in a dark room.

Photosensitization

Cells (2×10^4 cells/well in 96-well plates or 3×10^6 cells/6 cm plates) were plated and cultured overnight. To start the experiment, the cells were preincubated with the indicated concentrations of Pd-Bchl-Ser (4 hours, 37°C), illuminated and further incubated as indicated in the individual experiments. Dark controls were treated with sensitizer but not illuminated, while light controls were illuminated in the absence of sensitizer.

Cell survival assay

Neutral red assay

Following photosensitization and a 24-hour incubation in the culture incubator (37°C), cell survival was determined by neutral red (Fluka Chemie, Buchs, Switzerland) accumulation as described previously (Borenfreund and Puerner, 1985). After subtraction of assay blanks, net optical density (570 nm) was computed as the average value of triplicate determinations. Cell survival was calculated as the percentage of the dye accumulated in the untreated controls.

Propidium iodide assay

Following photosensitization, cells were rinsed twice with phosphate-buffered saline (PBS) and treated with 0.25 μg/ml propidium iodide (PI) (Sigma Chemical Co., St Louis, MO) (37°C, 15 minutes) (Tas and Westerneng, 1981). Cells were then rinsed twice in PBS, to

remove excess PI, and observed by fluorescence microscopy using a Rhodamine filter.

Fluorescence microscopy

Cells were observed and photographed with either an inverted fluorescence microscope (Zeiss Axiovert 35, Oberkochen, Germany) or with an upright fluorescence microscope (Nikon Corporation, Tokyo, Japan) both equipped with a digital camera (DVC, Austin, TX).

Video microscopy

An Applitec CCD camera and LIS 700 frame grabber were connected to a Zeiss Axiovert 35 microscope. Real-time videos were recorded on a Panasonic VCR (AG-7355). Still photographs of the indicated times were prepared from the real-time videos on a Macintosh platform with a built-in AV card using NIH Image 1.62. ImageJ 1.330 software (PC) by Wayne Rasband was used for image analysis.

Selected frames from the videos were extracted and presented in sequence to allow for monitoring of single cells and their time-dependent morphological changes.

Image analysis

Cell shape/morphology was determined by evaluation of cell circularity computed as $circularity=4\pi \times (area)/perimeter^2$. Circularity values vary from 1 (for a perfect circle) to 0. Values below 1 indicate an elongated or stellate cell body and/or an increasing number of cellular processes (Berezin et al., 1997; Bard et al., 2003). For graphic presentation, normalized mean values ± s.e.m. of circularity of randomly chosen cells in each group were plotted. For determination of cell motility, the tracks of single, randomly chosen cells were followed using the centroid (cell body center) as reference. For each plot, the paths of the cells were measured, normalized and converted to wind rose plots where the starting position of each cell (X-Y) was translated to start from (0,0) in the coordinate system (Fisher et al., 1989). In addition, total cell displacement was calculated by measuring the change in position of the cell centroid every 30 minutes over a period of 150 minutes. An average of total cell displacement for the randomly chosen cells in each group was calculated.

Detection of photogenerated ROS

Determination of specific ROS production following photosensitization of Pd-Bchl-Ser was carried out by spectral analysis of the oxidation products of hydroethidine (HE) (Molecular Probes, Eugene, OR) under cell-free and cell culture conditions. The oxidation products of HE include ethidium (E^+) (Bucana et al., 1986) and a unique monooxygenated superoxide/HE product (mHE) (Zhao et al., 2003), which become fluorescent upon intercalation with nuclear DNA.

Cell-free spectrofluorometric analysis

Superoxide

Pd-Bchl-Ser (2.5 μM) was mixed with HE (50 μM), salmon testes DNA (220 μg; Sigma Chemical Co.) and diethylenetriamine pentaacetic acid (DTPA) (100 μM) in PBS at a final volume of 1 ml. To initiate photogeneration of ROS, the mixtures were then illuminated (5 minutes, 20 mW/cm^2). Identification of superoxide was carried out as described by Zhao et al. (Zhao et al., 2003).

Hydroxyl radical

The reaction was carried out in the same manner, and respective contribution of superoxide and hydroxyl radical to the overall pool of generated radicals was resolved by respective addition of superoxide dismutase (SOD; Sigma Chemical Co.) or melatonin (Sigma Chemical Co.) at the indicated concentrations. The contribution of hydroxyl radical to the signal was estimated from the differential scavenging effects of SOD and melatonin.

To simulate the membrane lipid environment, 1.5% Triton X-100 was used as solvent in place of PBS.

Fenton reaction

The classical Fenton reaction was used to generate hydroxyl radicals under cell-free conditions. $FeSO_4$ (1 mM) and H_2O_2 (1 mM) were reacted in the presence of 50 μM HE and 220 μg DNA in a final volume of 1 ml PBS.

For detection of the oxidation products, samples were excited at 480 nm with a 4 nm slit and the spectra were recorded over the wavelength region of 550-750 nm using an 8 nm slit (emission max at 604 nm for ethidium and 580-590 nm for mHE). A solution containing 60 μM ethidium bromide and 220 μg/ml salmon testes DNA was used as reference. Fluorescence spectra were recorded on a SLM-AMINCO MC200 monochromator fluorospectrometer.

Spectroscopic analysis in cultured cells

For determination of intracellular ROS production, mouse M2R melanoma cell monolayers were preincubated (4 hours, 37°C in culture medium) with 100 nM Pd-Bchl-Ser, rinsed with PBS (37°C) to remove extracellular sensitizer, treated with 10 μM HE in PBS and illuminated immediately thereafter for varying lengths of time (0.5-10 minutes). Cells were then rinsed twice with PBS (37°C) and collected into 1 ml PBS for spectrofluorometric analysis as described above. As reference for ethidium fluorescence, untreated cells were collected and mixed with 60 μM ethidium bromide.

Flow cytometry

ROS generation was detected upon incubation of cells with varying concentrations of Pd-Bchl-Ser (4 hours, 37°C), which were then incubated (10 minutes, 37°C) with either 2 μM HE for detection of superoxide and hydroxyl radical, or with 10 μM of the nonfluorescent fluorochrome 2′,7′-dichlorodihydrofluorescein diacetate (H_2DCFDA) (Sigma Chemical Co.) to detect general ROS. The latter reagent is de-esterified intracellularly and becomes highly fluorescent upon oxidation to 2′,7′-dichlorofluorescin (DCF) (LeBel et al., 1992). For photosensitization, the cells were then illuminated (10 minutes, 20 mW/cm^2). The treated cells were subsequently trypsinized, collected and washed in PBS, and fluorescence was determined by excitation at 488 nm and emission at wavelengths 580±21 nm for HE and 530±15 nm for DCF, using the FACScan with Cellquest software (Beckton-Dickinson FACScan, San Jose, CA).

Preparation and analysis of cell lysates

Cell extracts were prepared in RIPA lysis buffer (Yung et al., 2001), subjected to SDS-PAGE and proteins were immunodetected on nitrocellulose membranes using anti-phosphorylated p38, ERK, JNK (Sigma Chemical Co.) or Akt (Cell Signaling Technology, Beverly, MA) antibodies and anti-p38 or ERK (Sigma Chemical Co.) antibodies.

Immunoprecipitation and kinase activity

Anti-phosphorylated-p38 was bound to packed Affi-prep protein A support beads (Bio-Rad Laboratories, Hercules, CA). Beads were then washed with PBS and cold buffer A (Yung et al., 2001) containing 1 mM DTT. Packed beads were mixed (1:1) with buffer H (buffer A + 1 mM benzamidine, 10 μg/ml aprotinin, 10 μg/ml leupeptin, 10 μg/ml pepstatin A) and were gently rotated with the cell extracts (2 hours,

4°C) to allow for adsorption of p-p38. The suspension was washed as described previously (Yung et al., 2001) and the immunoprecipitated p38 proteins were tested for activity using [γ-^{32}P]ATP and myelin basic protein (MBP) as substrates (Jaaro et al., 1997). The reaction was stopped with sample buffer and heating (5 minutes, 95°C). Samples were subjected to SDS-PAGE and radioactivity was monitored by autoradiography on X-ray film.

Immunofluorescent cell staining

Cells cultured on glass coverslips were fixed with 3% paraformaldehyde (PFA), postfixed and permeabilized in 3% paraformaldehyde and 0.5% Triton X-100 and blocked with 2% bovine serum albumin (BSA) and 2% normal goat serum (NGS). Cell samples were incubated with mouse anti-phosphorylated-p38 (with or without the doubly phosphorylated p38 peptide immunogen (Sigma Chemical Co.) prereacted (5:1, 2 hours) with anti-phosphorylated p38) or rabbit anti-p38. Samples were then blocked again and reacted with Cy3-conjugated goat anti-mouse IgG (Jackson ImmunoResearch Laboratories, Inc., Westgrove, PA) or Cy3-conjugated goat anti-rabbit IgG (Jackson ImmunoResearch Laboratories, Inc.) and mounted in elvanol on glass slides. Cells were photographed with an upright fluorescence microscope.

All experiments in this study were conducted at least three times and representative experiments are presented.

Results

The phototoxic efficacy of Pd-Bchl-Ser on cultured M2R cells

To establish the efficacy of the photoswitch, the photocytotoxicity of in-situ-illuminated Pd-Bchl-Ser was determined in cultured M2R cells. Cell cultures were preincubated with increasing concentrations (0-1000 nM) of sensitizer, illuminated for 10 minutes or not illuminated and cell viability was determined using the neutral red protocol (Fig. 1). Cell survival declined with increasing concentrations of Pd-Bchl-Ser in illuminated cultures with a median lethal dose (LD_{50}) ≈ 30 nM. In contrast, dark controls were hardly affected by Pd-Bchl-Ser in the same concentration range. This cell survival curve was used to determine the LD_{90} (100 nM) that was used in all subsequent experiments for inducing extensive cell death, while 15 nM Pd-Bchl-Ser were used for experiments at LD_{20}, in which generation of mild ROS challenge was required.

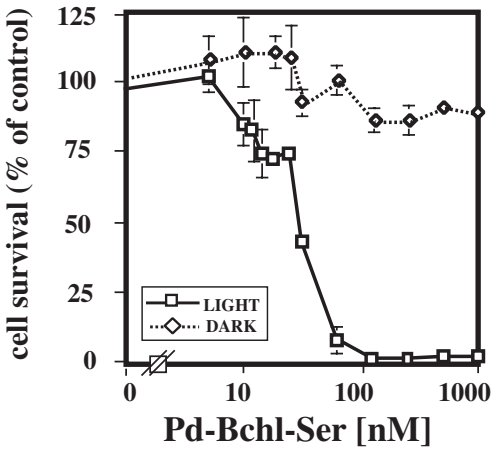

Fig. 1. Photosensitization of Pd-Bchl-Ser: effect on cell survival. M2R cells (4×10^4 cell/well) grown in 96-well plates were preincubated with increasing concentrations of Pd-Bchl-Ser, and either illuminated (light) or not illuminated (dark). Cells were then reincubated for 24 hours in the culture incubator and cell survival was determined using the neutral red assay. Points represent means of triplicate determinations ± s.d.

ROS generation upon photosensitization of Pd-Bchl-Ser

To correlate the above concentration-dependent cytotoxicity of the sensitizer with light-dependent production of ROS, determination of the specific species that evolve upon photosensitization under physiological conditions was monitored. Using ESR-based methods we previously demonstrated the photogeneration of superoxide and hydroxyl radicals by Pd-bacteriochlorophyll derivatives under nonphysiological conditions (Vakrat-Haglili et al., 2005). Fluorescence-based detection of ROS in cultured cells with HE has been reported by others (Bucana et al., 1986). However, specific intracellular identification of superoxide with HE has only recently been reported (Zhao et al., 2003). These authors showed that oxidation of HE to the two-electron oxidized ethidium (E^+) can be achieved by a variety of oxidants, however, only O_2^- yields a mono-oxygenated (mHE) product with unique spectral properties (max emission 580 nm). This method was employed here to allow for the detection of O_2^- generation under mild physiological concentrations in cell-free and cellular models. As shown below we extended this method to also determine the presence of hydroxyl radicals.

Oxidation of HE in cell-free studies

To determine ROS generation upon photosensitization of Pd-Bchl-Ser, cell free conditions were examined first. Pd-Bchl-Ser was incubated with DNA and HE in PBS. Samples were illuminated and fluorescence emission was recorded upon excitation at 480 nm. An increase in fluorescence emission of mHE at 580 nm in the presence of DNA was detected, demonstrating a clear shift from the E^+ standard fluorescence peak seen at 605 nm (Fig. 2A). Identification of O_2^- as the precursor of this shift, relied on the observed attenuation of the mHE fluorescence signal by ~90% upon the addition of superoxide dismutase (SOD) to the reaction mixture (Fig. 2A). It was thus concluded that superoxide is the major oxidant formed by photosensitization of Pd-Bchl-Ser in PBS.

In an attempt to simulate the cytosol/membrane interface, the above photoexcitation of Pd-Bchl-Ser was carried out in a two-phase micellar system consisting of 1.5% Triton X-100 in PBS, providing more favorable conditions for ROS generation (Vakrat-Haglili et al., 2005). Indeed, under these conditions, the fluorescence of the mHE product, dramatically increased where the signal was only slightly inhibited by SOD but significantly quenched by addition of the hydroxyl radical scavenger melatonin (Fig. 2B), indicating that the hydroxyl radical is the major component yielding this signal at the micelle interface.

This observation raised the possibility that in addition to superoxide, as reported earlier (Zhao et al., 2003), HE can also be partially oxidized to mHE by hydroxyl radicals. To test this hypothesis, the classical Fenton reaction was used to generate hydroxyl radicals under cell-free conditions. $FeSO_4$ (1 mM)

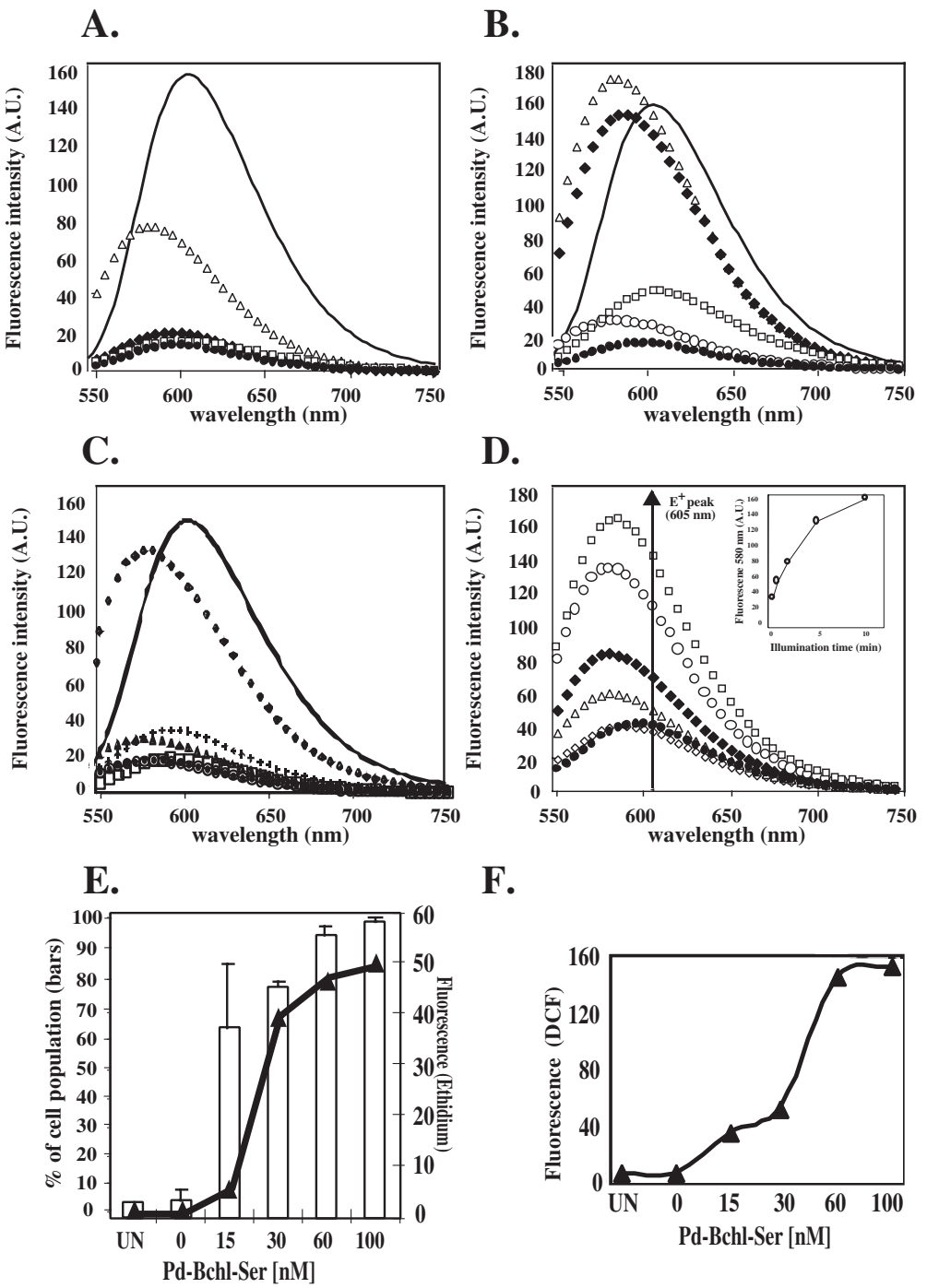

Fig. 2. Induction of ROS generation within cells upon photosensitization with Pd-Bchl-Ser and light. Cell-free spectroscopic analysis (A) 2.5 μM Pd-Bchl-Ser were incubated with 50 μM HE, 220 μg DNA and 100 μM DTPA in 1 ml PBS (open triangles) and then illuminated for 5 minutes at 20 mW/cm^2. Controls: dark control (closed circles) was not illuminated; illuminated samples with SOD (6×10^3 U; closed diamonds). Basic fluorescence in the illuminated sample was determined in the absence of DNA (open squares), or ethidium standard containing DNA and 60 μM ethidium bromide (solid line). Fluorescence intensity was then determined upon excitation at 480 nm with a slit width of 4 nm and an emission slit width of 8 nm. (B) As in A, but samples were prepared in 1.5% Triton X-100 and an additional control containing 8 mM melatonin was included (open circles). When added, SOD concentration was 100 U/ml (closed diamonds). (C) Fenton reaction: 1 mM H_2O_2 was incubated with $FeSO_4$ at a 1:1 molar ratio in the presence of 50 μM HE and 220 μg DNA in a final volume of 1 ml PBS (closed diamonds) and fluorescence was determined as in A. Controls: reaction mixture with 1 mM H_2O_2 and 1 mM $FeSO_4$ in the presence of 24 mM melatonin (closed circles), with 3 mM H_2O_2 without $FeSO_4$ (closed triangles), with 3 mM $FeSO_4$ without H_2O_2 (crosses) or with HE alone (open squares), ethidium bromide and DNA as in A. (D) Oxidation of HE in cultured cells. M2R cells were preincubated with 100 nM Pd-Bchl-Ser, rinsed and medium replaced with 10 μM HE in PBS. Cells were illuminated immediately thereafter for 0.5 (open diamonds), 1 (open triangles), 2 (closed diamonds), 5 (open circles) or 10 (open squares) minutes and collected for determination of fluorescence emission. Dark control was treated with HE for 10 minutes in the dark (closed circles). Graph insert illustrates fluorescence maxima at 580 nm as a function of time. (E) M2R cell monolayers were preincubated with 0, 15, 30, 60 or 100 nM Pd-Bchl-Ser for 4 hours and then treated with 2 μM HE for 10 minutes and illuminated prior to FACS analysis. Bars represent the percentage of cells emitting fluorescence following treatment and the graph represents the fluorescence intensity. (F) M2R cells were preincubated with 0, 15, 30, 60 or 100 nM Pd-Bchl-Ser for 4 hours and then treated with 10 μM H_2DCFDA for 10 minutes and illuminated prior to FACS analysis.

and H_2O_2 (1 mM) were reacted in the presence of HE and DNA. A distinct shift in HE fluorescence, similar to that described for superoxide-based oxidation of HE was observed but was fully quenched in the presence of melatonin and thus ascribed to hydroxyl radicals (Fig. 2C). Consequently, these results suggest that HE can be oxidized to mHE by hydroxyl radicals as well and that photosensitization of Pd-Bchl-Ser generates both superoxide and hydroxyl radicals in a micellar environment. The above ROS profile obtained in aqueous and micellar conditions support earlier ESR-based analyses carried out in our laboratory (Vakrat et al., 1999; Vakrat-Haglili et al., 2004 submitted). However, in contrast to the ESR method, the HE-based method allows for detection of ROS at much higher sensitivity, permitting analysis at physiological concentrations

in both cell-free and cell culture models as demonstrated below.

Oxidation of HE in cultured cells

In attempt to identify intracellularly generated ROS using this method, we next examined photosensitization of Pd-Bchl-Ser-treated M2R cells in the presence of HE. M2R cells were preincubated with Pd-Bchl-Ser (100 nM, 4 hours, 37°C), washed to remove free sensitizer, treated with 10 μM HE in PBS and subsequently illuminated for increasing time intervals (0.5-10 minutes). Fluorescence emission at 580 nm was recorded upon excitation of the cell suspension at 480 nm. A positive correlation was observed between the fluorescence intensity of mHE and the light dose delivered over increasing photosensitization times (0-10 minutes) (Fig. 2D), demonstrating maintained ROS generation throughout the illumination period. Based on the above results, we suggest that both superoxide and hydroxyl radicals are differentially generated in the cytosol and cytosol/membrane interface. However, in the absence of information concerning the subcellular partitioning of Pd-Bchl-Ser, along with the intricacy of treating cells with type-specific antioxidants, conclusive results regarding the ratio between the intracellularly generated ROS awaits further development of appropriate experimental tools.

Flow cytometric analysis

ROS generation as a function of Pd-Bchl-Ser concentrations was further determined by flow cytometry in the presence of HE or 2′,7′-dichlorodihydrofluorescein (H_2DCF), a common ROS reporter molecule. While untreated and light control cells showed minimal fluorescence signals, fluorescence intensity rose with increasing sensitizer concentrations, signifying increased cellular ROS production that reached maximal levels upon treatment with >60 nM Pd-Bchl-Ser for HE (Fig. 2E) and 2′,7′-dichlorofluorescein (DCF) (Fig. 2F). Upon challenge with 15 nM sensitizer (LD_{20}), fluorescence levels attained ~10 and 25% of the respective maximal levels. Furthermore, the photosensitization of Pd-Bchl-Ser appears to take place in the majority of the cell population, as demonstrated by oxidation of HE. While fluorescence intensity over the tested range rose nearly tenfold, the percentage of fluorescently labeled cells following treatment varied by only 30% (Fig. 2E). Thus, we can conclude that cellular ROS generation is achieved in the majority of the cells and not merely in a hypersensitive fraction of the population.

Determination of cell fate following photosensitization of M2R cells with Pd-Bchl-Ser at LD_{90} and LD_{20}

In order to determine at which point photosensitized cells undergo irreversible membrane damage and become committed to death, cell viability was determined using propidium iodide (PI) (Fig. 3). Nuclear PI staining was apparent immediately after illumination of the cells in the presence of LD_{90} sensitizer concentrations, gradually intensifying with time to cover the entire nucleus by 24 hours after treatment. Along with this process, changes in cell morphology were observed with apparent cell disintegration by

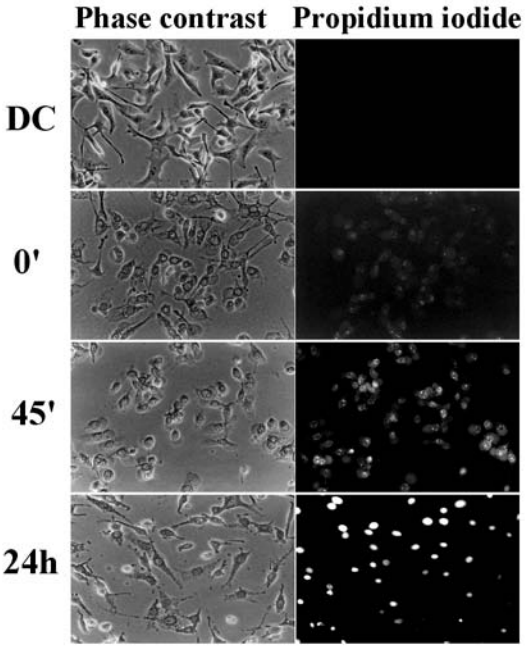

Fig. 3. Commitment to death after treatment with Pd-Bchl-Ser and light. M2R cells were preincubated with Pd-Bchl-Ser at LD_{90} (DC) and then illuminated, reincubated (0 minutes, 45 minutes and 24 hours) and then stained with PI. Time points indicate the incubation time following illumination excluding the 15 minutes staining process. Phase-contrast microscopy is presented in the left column and fluorescence microscopy with PI staining is presented in the right column.

24 hours (Fig. 3, phase-contrast images). In contrast, no PI staining and no morphological changes were observed, for up to 2 hours after illumination, in cells treated in the same manner at LD_{20} (not shown). Neither dark controls (LD_{90}) nor untreated cells (not shown) gave any PI signal. These results suggest that commitment to death occurs within the illumination time window at LD_{90} while cell viability is largely maintained at LD_{20}.

Morphological changes induced in M2R cells following photosensitization with Pd-Bchl-Ser

Owing to the established role ROS play in cellular responses, including proliferation (Preston et al., 2001; Kim et al., 2001), differentiation (Finkel, 2000), motility/invasiveness (Mori et al., 2004) and apoptosis (Gotoh and Cooper, 1998; Ichijo et al., 1997), we chose to monitor the induced changes in cell morphology/motility following ROS challenge. To avoid loss of information on morphological changes that may result from use of still photography, individual photosensitized cells were continuously monitored by video microscopy. Upon photosensitization at LD_{90}, cells underwent irreversible morphological changes leading to cell shrinkage or lysis (Fig. 4A, LD_{90}), in agreement with the observations of phase photography (Fig. 3). In contrast, we observed stimulated motility of the cells following photosensitization at LD_{20}, where total cell displacement was twofold higher (D=46 μm versus 25 μm) than in untreated and light control groups (Fig. 4B). Although cell morphology appeared typical, upon

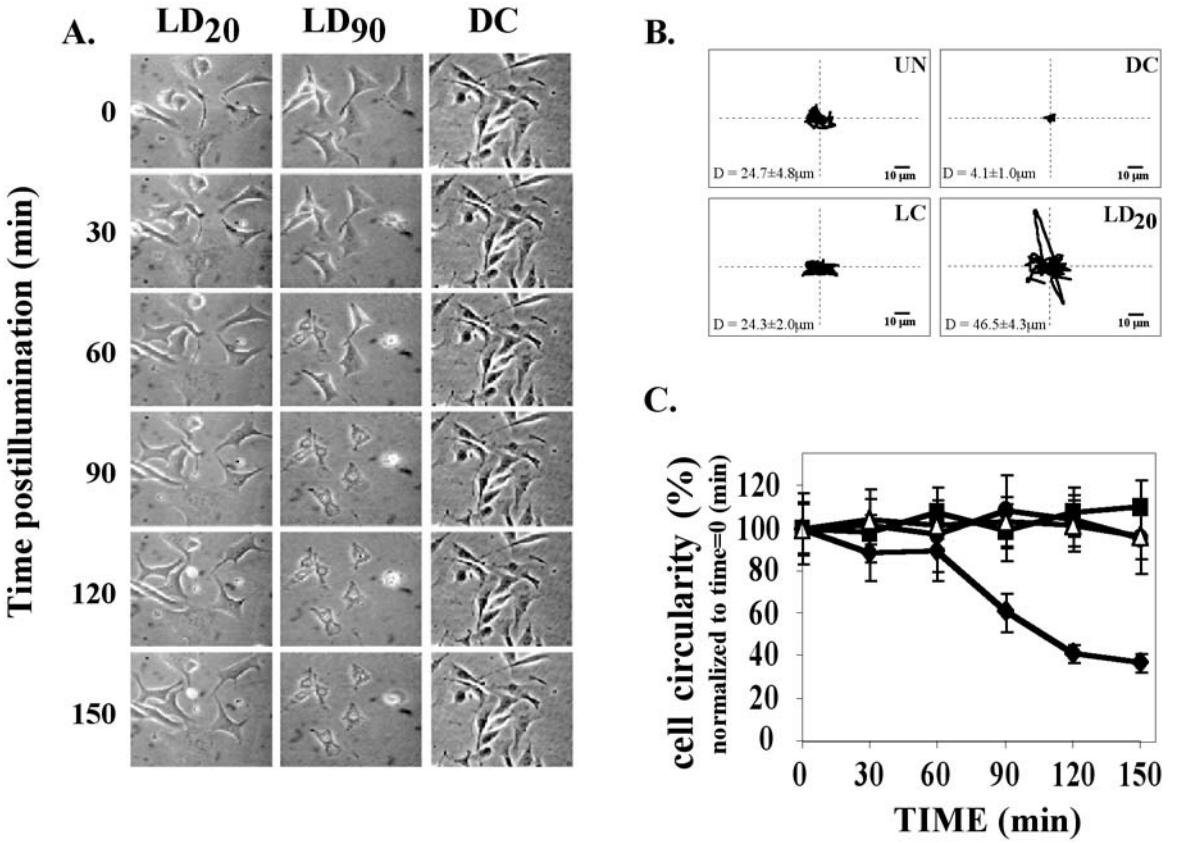

Fig. 4. Morphological changes in M2R cells following treatment with Pd-Bchl-Ser and light. (A) M2R cells were treated at LD_{90} with no illumination (dark controls), LD_{90} and illumination (LD_{90}) or LD_{20} and illumination (LD_{20}) and selected groups of cells were continuously monitored over a 2.5-hour period using video microscopy. Videos were processed and the still photographs of indicated times are presented. By following individual cells throughout the frames, one can observe cell motility by following the morphological changes of particular cells over time. (B) For each plot, the paths of ten cells were measured, normalized and converted to wind rose display where all cells start from (0,0) in order to illustrate the average motility. UN, untreated; DC, dark control; LC, light control; LD_{20}, LD_{20} treatment. Total cell displacement was calculated by measuring the change in position of the cell centroid every 30 minutes over a 2.5-hour period. An average of total cell displacement (D) ± s.e.m. for 10 randomly chosen cells in each group was calculated and is presented in the respective rose wind plot. Total displacement of LD_{20}-treated cells in comparison to other experimental groups were significantly different (P values <0.0005). (C) Cell circularity was computed as $circularity=4\pi \times (area)/perimeter^2$. Normalized average ± s.e.m. of circularity of 10 randomly chosen individual cells in each group were plotted. Untreated (closed squares), dark control (open triangles), light control (closed circles), LD_{20} treatment (closed diamonds).

quantification of their circularity over time, a drastic decrease (from 100% to 37%) was observed following LD_{20} treatment, representing an increase in the number of cellular processes (Fig. 4C). Untreated and light controls exhibited a basal level of motility while overall cell circularity was preserved (Fig. 4B,C), whereas cell motility was essentially absent in dark controls (Fig. 4A-C). These results suggest that mild ROS challenge enhances cell motility and dispersion without causing significant cell death.

Phosphorylation and activation of p38 MAPK in M2R cells following photosensitization of Pd-Bchl-Ser (LD_{90})

In order to examine the effects of ROS on specific enzymatic processes, cells were treated with Pd-Bchl-Ser at LD_{90}. They were then immediately lysed and phosphorylated p38 MAPK (p38) levels were determined using western blot analysis. An abrupt rise in phosphorylated p38-α levels was observed (Fig. 5A) from an almost negligible basal level in untreated cells. Light and dark controls displayed no elevation of phosphorylated p38.

To determine if the phosphorylated p38 was catalytically active, immunoprecipitates of phosphorylated p38 were examined for kinase activity using [γ-^{32}P]ATP and MBP as substrates. Photosensitization of Pd-Bchl-Ser was found to catalytically activate p38 immediately following treatment (Fig. 5B), in correlation with phosphorylation of the enzyme. The slight increase in kinase activity in the light control, may result from photosensitization of endogenous pigments in this melanoma cell line.

The effect of photosensitization of Pd-Bchl-Ser (LD_{90}) on phosphorylation of p38, ERK, JNK and Akt

Time dependence

We next monitored the time course and selectivity of the phosphorylation of p38 and other protein kinases in M2R cells following treatment with Pd-Bchl-Ser and light. The effects of

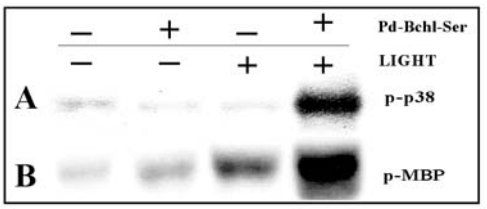

Fig. 5. Phosphorylation and stimulation of catalytic activity of cellular p38 following photosensitization with Pd-Bchl-Ser. M2R cells were preincubated with Pd-Bchl-Ser at LD_{90} and illuminated, and cell lysates were prepared immediately thereafter. (A) Proteins (30 μg protein/lane) were separated by 10% SDS-PAGE and detected with anti-phosphorylated-p38 antibody by immunoblotting. (B) Immunoprecipitation of p38 with anti-phosphorylated p38 was performed using the respective cell lysates. Catalytic activity of p38 was assayed using myelin basic protein (MBP) and [γ-^{32}P]ATP as substrates. Lysates were analyzed by autoradiography following SDS-PAGE. Detected bands show ^{32}P coinciding with position of MBP.

ROS upon the phosphorylation states of p38, extracellular signal-regulated kinase (ERK), c-Jun N-terminal kinase (JNK) and Akt were determined in cell lysates prepared over a 2-hour period following photosensitization of Pd-Bchl-Ser at LD_{90} (Fig. 6). As can be seen, p38-α was phosphorylated immediately following illumination and reached maximal levels within 100 minutes. JNK underwent a similar time-dependent phosphorylation. In contrast, ERK, which was phosphorylated in resting cells (Fig. 6, 0 minutes), underwent rapid dephosphorylation during the illumination step and was slowly rephosphorylated to close to its basal level within 2 hours. Similarly, Akt was dephosphorylated during the illumination step but remained so to the end of the experiment (Fig. 6). In comparison to zero time, no effect was seen in dark control cells that had been incubated with Pd-Bchl-Ser at LD_{90} for 6 hours (Fig. 6). It was therefore concluded that in situ generation of lethal doses of ROS, following photosensitization of Pd-Bchl-Ser in M2R cells, affects the four selected protein kinases in a protein-specific and time-dependent manner, involving both phosphorylation (p38, JNK) and dephosphorylation (ERK, Akt). It was noted that cessation of illumination did not instantly reverse the induced changes in phosphorylation levels and that the general trends induced were maintained over extended periods.

Sensitizer concentration dependence

To further analyze the response of these protein kinases to different ROS levels, cells were pretreated with increasing concentrations of Pd-Bchl-Ser and then illuminated at a constant light dose. Cell lysates were prepared 45 minutes postillumination and the phosphorylation states of p38, ERK, JNK and Akt were determined. As illustrated in Fig. 7, ERK was dephosphorylated following illumination even at low (8 nM) photosensitizer concentrations. Phosphorylation of p38-α and JNK was observed with increasing Pd-Bchl-Ser concentrations, >8 nM and >15 nM, respectively. In contrast, Akt showed a decline in phosphorylation levels only following severe ROS challenge. These data illustrate that the tested protein kinases exhibit varying levels of sensitivity to ROS and demonstrate individual response patterns to the stress induced by photosensitization of increasing concentrations of Pd-Bchl-Ser. It was noted that kinase activities were affected at low sensitizer levels and in the case of p38 and ERK even in response to mild ROS challenge.

Phosphorylation of p38 and ERK following photosensitization with Pd-Bchl-Ser at mild doses: time dependence

In order to examine the possibility of stimulating enzyme activity following treatment of cells with moderate ROS concentrations, M2R cells were photosensitized at LD_{20} and the response of p38 and ERK was monitored as a function of time. ERK was observed to first become gradually dephosphorylated during the illumination period and through the first 25 minutes of treatment, and to then steadily become rephosphorylated over the next 100 minutes, reaching a final phosphorylation level that

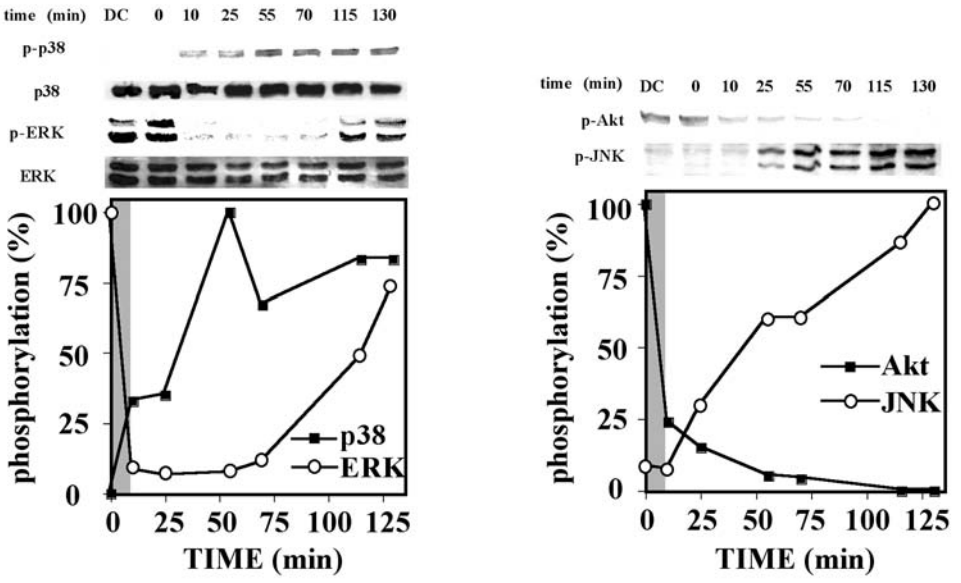

Fig. 6. Phosphorylation of protein kinases following treatment with Pd-Bchl-Ser at LD_{90} and light. M2R cell lysates were prepared at the indicated times following treatment. Proteins (75 μg protein/lane) were separated on 10% SDS-PAGE, blotted and immunodetected with anti-phosphorylated p38, ERK, JNK or Akt. Resting levels of phosphorylated protein kinases were determined on untreated (0 minutes) cells. Dark controls (DC) were treated with sensitizer but not illuminated. Blots reacted with anti-p38 and anti-ERK measured total amounts of protein blotted. Graphs represent relative phosphorylation of proteins as a percentage of the band density displaying the highest value on the given blot. The gray area denotes the duration of the illumination.

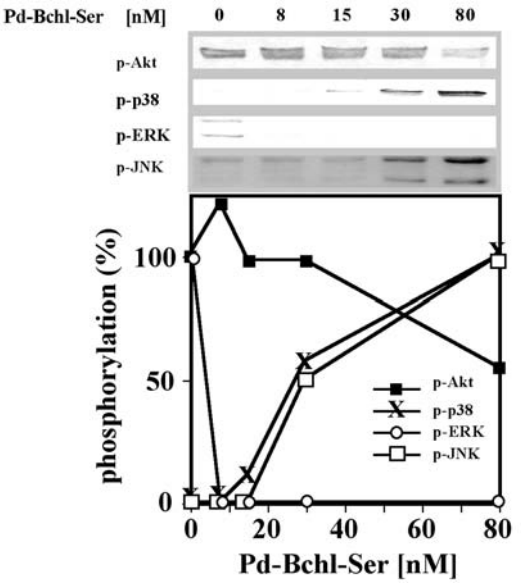

Fig. 7. Phosphorylation of protein kinases following treatment with light and increasing concentrations of Pd-Bchl-Ser. Cells were preincubated with increasing concentrations of Pd-Bchl-Ser, illuminated for 10 minutes and reincubated for 45 minutes. Cell lysates were prepared and proteins were separated on 10% SDS-PAGE, blotted and immunodetected with anti-phosphorylated p38, ERK, JNK or Akt. Phosphorylation is presented as a percentage of the band density displaying the highest value on the respective blot.

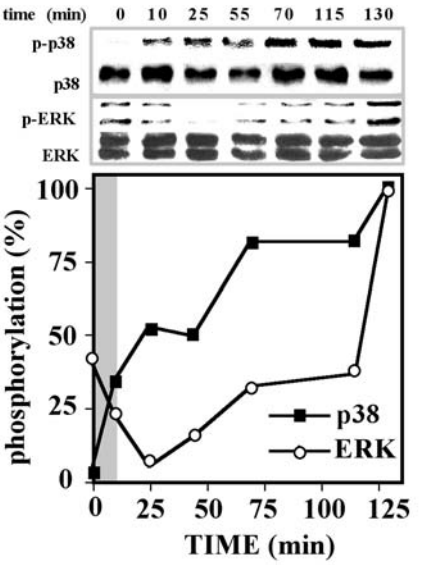

Fig. 8. Phosphorylation of protein kinases following treatment with Pd-Bchl-Ser at LD_{20} and light. M2R cell lysates were prepared at the indicated times following treatment. Proteins (75 μg protein/lane) were separated on 10% SDS-PAGE, blotted and immunodetected with anti-phosphorylated p38 or ERK. Resting levels of phosphorylated protein kinases were determined on untreated (0 minutes) cells. Blots reacted with anti-p38 and anti-ERK measured total amounts of protein blotted. The graph represents relative phosphorylation of proteins as percent of the band density displaying the highest value on the given blot. The gray area denotes the illumination time interval.

was about twice that seen at resting levels (Fig. 8). In contrast, phosphorylation of p38-α was initiated within the illumination window and its levels gradually increased with time. These findings indicate that similar to the effects observed following lethal ROS challenge, mild sensitizer concentrations induce similar profiles of prolonged changes in the phosphorylation levels of ERK and p38-α, and in the case of p38, stimulate its catalytic activity as well (Fig. 5B).

Changes in the subcellular distribution of phosphorylated p38 following photosensitization of M2R cells with Pd-Bchl-Ser at LD_{90} and LD_{20}

In order to determine if ROS-induced p38 activation is confined to specific subcellular compartments, cells were treated with Pd-Bchl-Ser at LD_{90} or LD_{20}, fixed at varying time intervals thereafter (0-90 minutes) and then stained for phosphorylated-p38. It was found that although p38 was distributed throughout the resting cell (Fig. 9A, UN-p38), the phosphorylated, active form of the enzyme was confined mainly to the cell nucleus (Fig. 9A,B, UN). An abrupt rise in phosphorylated p38 levels was seen in both the nucleus and cytoplasm (Fig. 9A) immediately following ROS challenge at LD_{90} concentrations and remained relatively stable for 45 minutes. Similarly, when cells were treated with mild ROS doses, phosphorylated p38 levels rose in both the nucleus and cytoplasm (Fig. 9B) and remained high for the entire 90 minutes of observation. The elevation of phosphorylated p38 levels noted in the cells' cytoplasm might represent p38 activated from the cytoplasmic pool or p-p38 that was translocated from the nucleus (Ben-Levy et al., 1998).

Discussion

The classical interpretation of ROS as detrimental agents leading to indiscriminate destruction of cellular components, has been reconsidered following the observed consequences of mild ROS challenge inducing nonlethal biochemical and morphological changes in cells (Adler et al., 1999b; Finkel, 2000; Kamata and Hirata, 1999; Remacle et al., 1995; Suzuki et al., 1997). This study shows that photosensitization of Pd-Bchl-Ser-treated cells can differentially generate superoxide and hydroxyl radicals, depending on the sensitizer's microenvironment (Fig. 2A,B). Furthermore, ROS levels increased with increasing sensitizer concentrations in a light- and time-dependent manner, as shown with two independent methods using HE and DCF as reporters (Fig. 2). Moreover, this study demonstrates a tight causal relationship (Fig. 10) between ROS production and ensuing cellular responses (Figs 1, 2, 7). We illustrate that this system can be utilized as a manipulable photoswitch, allowing for simple and tightly controlled exposure of cells to varying doses of ROS. Using this photoswitch, we provide new insights that correlate dose-dependent photogeneration of ROS with differential catalytic responses of several protein kinases and changes in their intracellular distribution, and also alterations in cell motility, morphology and viability. Thus, when also considering the positive correlation between ROS generation and increasing light doses (Fig. 2D), this photoswitch provides a dynamic means of determining the precise threshold of each catalytic response.

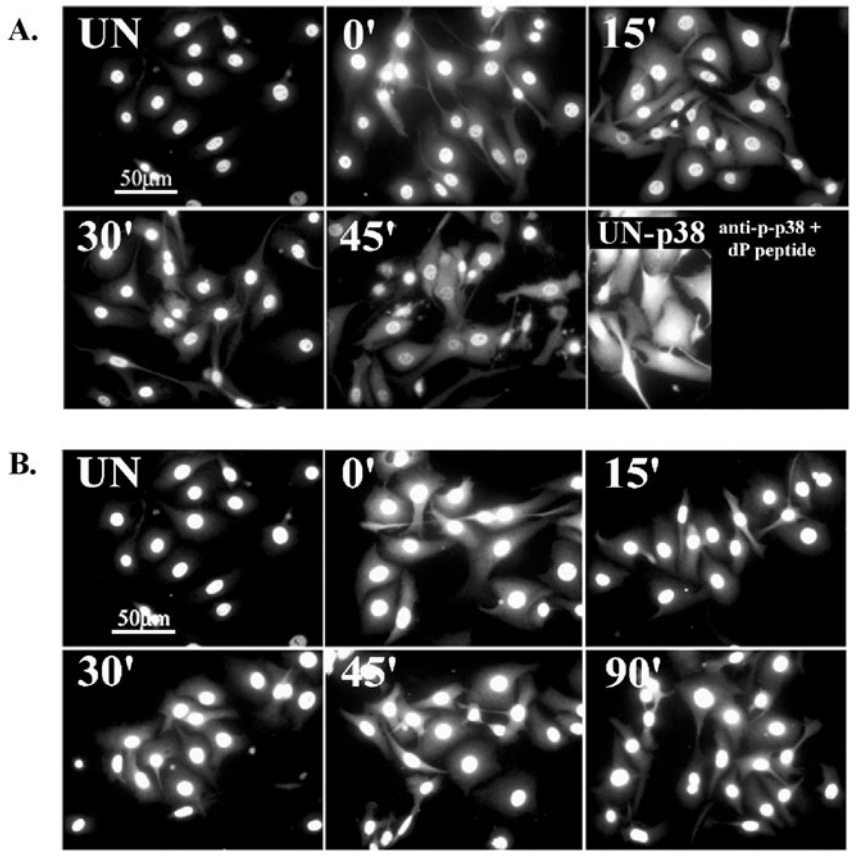

Fig. 9. Cellular location of p38 following treatment of M2R cells with Pd-Bchl-Ser and light. (A) Cells were treated with Pd-Bchl-Ser at LD_{90} and light. Samples were fixed and permeabilized at varying time intervals after illumination (0-45 minutes) and stained with anti-phosphorylated p38. UN, untreated cells; UN-p38, untreated cells stained with anti-p38; anti-p-p38+dP peptide, immunostaining of cells treated with anti-phosphorylated p38 pre-reacted with its immunogen, the doubly phosphorylated (dP) p38 peptide, was completely blocked demonstrating specificity of the staining. (B) As in A but cells were treated with Pd-Bchl-Ser at LD_{20} and light.

To date, typical protocols for exposure of cells to ROS utilize diffusible ROS (H_2O_2), ROS-generating drugs (anthracyclines) (Konorev et al., 1999) or ROS-generating enzymes (xanthine/xanthine oxidase) (Olszanecki et al., 2002) that are reactive immediately upon administration and their de novo ROS generation cannot be accurately initiated or easily terminated. The approach described here utilizes two inert components, a photosensitizer at various concentrations, which requires pre-accumulation, and matched, nonhazardous light, at varying energy doses delivered for precisely controlled times (fractions of a second) and at predetermined locations. Manipulation of both sensitizer concentrations and light doses allow for precise control of final ROS levels and achievable challenge intensities. Although the subcellular distribution of Pd-Bchl-Ser is not presently known, sensitizer targeting to distinct cellular regions can be obtained (Gross et al., 1997; Konan et al., 2002; Rosenkranz et al., 2000) and laser light may be delivered to discrete cellular compartments. In addition, various bacteriochlorophyll derivatives (Brandis et al., 2005; Scherz et al., 2000), bearing diverse physicochemical properties, can generate different ROS profiles, providing additional advantages to the photoswitch in the study of ROS in physiological processes. Overall, this study demonstrates that escalation of ROS doses enables identification of cellular responses ranging from quasi-physiological to lethal.

Free radical production in a two-phase PBS/TritonX-100 system was used to simulate a membrane/cytosol interface and demonstrated distinct ROS profiles when generated in aqueous (PBS) vs. micellar environments (Fig. 2A,B). Furthermore, the results suggest that in addition to superoxide (Zhao et al., 2003), oxidation of HE to mHE can be achieved by hydroxyl radicals, as shown in the case of the Fenton reaction (Fig. 2C), indicating broader applications for this method of ROS detection. The possibility of singlet oxygen detection under these conditions was also examined but has thus far not provided conclusive results (data not shown). When compared to ESR, where ROS detection requires micromolar sensitizer concentrations, the HE-based methodology is simpler, considerably more sensitive (detection at nanomolar sensitizer levels) because of fluorescence-based signals, and easily adaptable for examination of ROS production under physiologically relevant conditions in cell-free and cellular models. Bacteriochlorophyll-based sensitizers tend to aggregate at high concentrations, a phenomenon that affects their photochemical properties, providing another advantage of HE-based analyses of ROS generation.

Determination of the specific ROS generated within the cells by detection of oxidation of HE to mHE requires application of type-specific antioxidants (Fig. 2A,B), which is presently difficult to apply intracellularly. Overexpression of cellular antioxidants can disrupt the steady-state equilibrium of active oxygen species within the cell, leading to increased oxidative damage, as exemplified in the case of SOD overexpression which led to increased cellular H_2O_2 production and extensive lipid peroxidation (Elroy-Stein et al., 1988). Furthermore, it must be stressed that the sites of cellular ROS production in relation to the distribution of the scavenger/antioxidant, even if both are within the same compartment, may not always lead to their interaction because of the extremely short half-life, and thus, short radius of operation of ROS. Therefore, external intervention in the delicate but very tightly controlled and remarkably unforgiving equilibrium of intracellular ROS is a rather complex matter and has still not been resolved in this field of study.

A positive correlation between escalations in ROS levels and the phosphorylation/activity states and subcellular distribution of specific protein kinases (Figs 5-9) was clearly demonstrated, specifically regarding the two renowned stress-related p38 and JNK MAPKs (Fig. 10). The diverse enzymatic responses displayed individual kinetic patterns, which spanned the illumination (de novo ROS generation) and subsequent dark periods. Furthermore, trends in the phosphorylation of the tested enzymes were maintained over these periods (Figs 6-9)

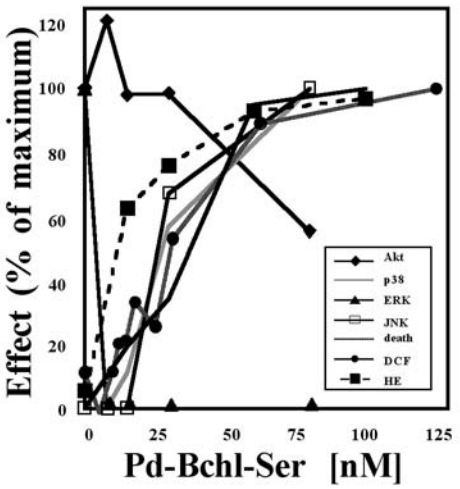

Fig. 10. Correlation between photosensitizer concentrations, ROS levels and respective cellular responses: The data presented in Fig. 2E,F (ROS production DCF, HE), Fig. 7 (phosphorylation levels of Akt, p38, ERK, JNK) and Fig. 1 (cell death) were converted to percentages of maximal effect, and expressed as a function of Pd-Bchl-Ser concentration.

possibly reflecting the effect of sequential free radical chain reactions (Gross et al., 2003; Koudinova et al., 2003) or a time-dependent recovery to the basal state. While, at lethal sensitizer levels, p38-α and JNK are phosphorylated, Akt is dephosphorylated and ERK shows a biphasic behavior (Fig. 6), after mild ROS challenge, only ERK and p38-α are affected in the same time period (Figs 8, 9). Although the majority of p-p38 was nuclear in the resting state and nonactive p38 was present throughout the cytoplasm, the activated enzyme was clearly observed in the cytoplasm upon photosensitization (Fig. 9). Whether this is dependent on nuclear transport of activated p38 to the cytoplasm or on ROS generation and direct activation of the pathway components within the cytoplasm, has yet to be determined. Earlier reports (Tao et al., 1996; Xue et al., 1999) linked activation of these enzymes to regulation of PDT-induced cell death. However, our results do not agree with this interpretation, as a similar pattern of activation of the same enzymes is also obtained following mild ROS challenge. Furthermore, the cells are already committed to death at termination of the illumination period (Fig. 3), and subsequent changes in enzyme activity can not reflect mediatory roles in the death process, but rather random cellular collapse that is morphologically visible over time (Figs 3, 4). However, under mild conditions, such ROS-induced changes appear to be reversible and therefore of potential physiological relevance. A suggested physiological consequence of chronic stimulation of epithelial cells with mild ROS doses has been recently reported to lead to heightened motility/invasiveness and eventual malignant cellular transformation (Mori et al., 2004). Moreover, our results clearly show that the biochemical, morphological and motility changes induced in cells by mild ROS challenge involve the majority of the cell population and not merely a fraction of hypersensitive cells (Fig. 2E, Fig. 4, Fig. 9B).

Differential sensitivity to ROS concentrations may allow for selective regulation of specific cellular activities at varying levels of stringency. For instance, cell cycle arrest induced by moderate levels of ROS (Barnouin et al., 2002) and induction of cell proliferation at lower doses have been described (Kim et al., 2001). The effects of ROS on protein kinase activity may have resulted from direct ROS influence on the specific enzyme analyzed. Yet, possible modification of enzymes located upstream or downstream to those studied must also be considered. It has been shown that protein tyrosine phosphatase is inactivated by H_2O_2 (Kamata et al., 2000) and in this manner involved in the regulation of the EGF receptor. Other studies suggest that ROS act as second messengers regulating protein kinases, partly via inactivation of protein phosphatases (Barrett et al., 1999; Kamata et al., 2000; Lee et al., 1998; Nemani and Lee, 1993; Robinson et al., 1999) and may even regularly act to keep certain brain phosphatases inactive (Floyd and Hensley, 2000). Alternatively, response of enzymes to changing redox states must also be considered. Molecules containing high thiol-disulfide oxidation potentials are most likely redox-sensitive and undergo conformational changes or form inter- or intramolecular disulfide bonds under oxidative conditions, transducing the cellular response to the altered redox conditions. Such redox-responsive proteins, including thioredoxin and glutathione S-transferase, have been characterized as regulators of p38 and JNK (Adler et al., 1999a; Ichijo et al., 1997) under stress-induced conditions.

The results of this study provide further experimental endorsement to the notion that ROS play a key role in initiation/mediation of a wide range of cellular responses via their effect on key enzymes of critical signaling pathways. Furthermore, we demonstrate that precise control of ROS photogeneration is feasible by subtle manipulation of sensitizer concentrations and light doses, a novel tool that allows for delicate regulation of ROS doses, type and compartmentalization as well as fine control of cellular exposure time to ROS challenge. In doing so, cells can be destined to death by lethal doses of ROS or can be physiologically manipulated while remaining viable. This observation forms the basis for future studies that will further enhance our understanding of the role of ROS in cellular signaling. The suggested approach of the photoswitch is expected to add a new dimension to the efforts of reaching this goal.

Y.S. is the incumbent of the Tillie and Charles Lubin Professorial Chair in Biochemical Endocrinology. A.S. is the incumbent of the Robert and Yadelle Sklare Professorial Chair in Biochemistry. All the studies described here were performed by Y.P. in partial fulfillment of her MSc and PhD theses requirements, The Feinberg Graduate School of the Weizmann Institute of Science. We thank Yahel Vakrat-Haglili for her instrumental help and Esther Shai for her help in the initial launching of this study and for her technical support. This research was supported by The Israel Science Foundation (grant no. 299/00-16.0).

References

Adler, V., Yin, Z., Fuchs, S. Y., Benezra, M., Rosario, L., Tew, K. D., Pincus, M. R., Sardana, M., Henderson, C. J., Wolf, C. R. et al. (1999a). Regulation of JNK signaling by GSTp. *EMBO J.* **18**, 1321-1334.

Adler, V., Yin, Z., Tew, K. D. and Ronai, Z. (1999b). Role of redox potential and reactive oxygen species in stress signaling. *Oncogene* **18**, 6104-6111.

Akhlynina, T. V., Jans, D. A., Rosenkranz, A. A., Statsyuk, N. V., Balashova, I. Y., Toth, G., Pavo, I., Rubin, A. B. and Sobolev, A. S.

(1997). Nuclear targeting of chlorin e6 enhances its photosensitizing activity. *J. Biol. Chem.* **272**, 20328-20331.

Ashur, I., Brandis, A., Greenwald, M., Vakrat-Haglili, Y., Rosenbach-Belkin, V., Scheer, H. and Scherz, A. (2003). Control of redox transitions and oxygen species binding in Mn centers by biologically significant ligands; model studies with [Mn]-bacteriochlorophyll a. *J. Am. Chem. Soc.* **125**, 8852-8861.

Bard, F., Mazelin, L., Pechoux-Longin, C., Malhotra, V. and Jurdic, P. (2003). Src regulates Golgi structure and KDEL receptor-dependent retrograde transport to the endoplasmic reticulum. *J. Biol. Chem.* **278**, 46601-46606.

Barnouin, K., Dubuisson, M. L., Child, E. S., Fernandez de Mattos, S., Glassford, J., Medema, R. H., Mann, D. J. and Lam, E. W. (2002). H_2O_2 induces a transient multi-phase cell cycle arrest in mouse fibroblasts through modulating cyclin D and p21Cip1 expression. *J. Biol. Chem.* **277**, 13761-13770.

Barrett, W. C., DeGnore, J. P., Keng, Y. F., Zhang, Z. Y., Yim, M. B. and Chock, P. B. (1999). Roles of superoxide radical anion in signal transduction mediated by reversible regulation of protein-tyrosine phosphatase 1B. *J. Biol. Chem.* **274**, 34543-34546.

Ben-Levy, R., Hooper, S., Wilson, R., Paterson, H. F. and Marshall, C. J. (1998). Nuclear export of the stress-activated protein kinase p38 mediated by its substrate MAPKAP kinase-2. *Curr. Biol.* **8**, 1049-1057.

Berezin, V., Skladchikova, G. and Bock, E. (1997). Evaluation of cell morphology by video recording and computer-assisted image analysis. *Cytometry* **27**, 106-116.

Berg, K. and Moan, J. (1997). Lysosomes and microtubules as targets for photochemotherapy of cancer. *Photochem. Photobiol.* **65**, 403-409.

Borenfreund, E. and Puerner, J. A. (1985). Toxicity determined in vitro by morphological alterations and neutral red absorption. *Toxicol. Lett.* **24**, 119-124.

Brandis, A., Mazor, O., Neumark, E., Rosenbach-Belkin, V., Salomon, Y. and Scherz, A. (2005). A. Novel water-soluble bacteriochlorophyll derivatives for vascular-targeted photodynamic therapy: synthesis, solubility, phototoxicity, and the effect of serum proteins. *Photochem. Photobiol*. (in press).

Bucana, C., Saiki, I. and Nayar, R. (1986). Uptake and accumulation of the vital dye hydroethidine in neoplastic cells. *J. Histochem. Cytochem.* **34**, 1109-1115.

Darrah, P. A., Hondalus, M. K., Chen, Q., Ischiropoulos, H. and Mosser, D. M. (2000). Cooperation between reactive oxygen and nitrogen intermediates in killing of Rhodococcus equi by activated macrophages. *Infect. Immun.* **68**, 3587-3593.

Davies, K. J. A. (1995). Oxidative stress: the paradox of aerobic life. In *Free Radicals in Oxidative Stress: Environment, Drugs and Food Additives* (ed. H. B. Evans C, Lunt GG). London: Portland Press.

Deora, A. A., Win, T., Vanhaesebroeck, B. and Lander, H. M. (1998). A redox-triggered ras-effector interaction. Recruitment of phosphatidylinositol 3′-kinase to Ras by redox stress. *J. Biol. Chem.* **273**, 29923-29928.

Devary, Y., Gottlieb, R. A., Lau, L. F. and Karin, M. (1991). Rapid and preferential activation of the c-jun gene during the mammalian UV response. *Mol. Cell. Biol.* **11**, 2804-2811.

Elroy-Stein, O. and Groner, Y. (1988). Impaired neurostransmitter uptake in PC12 cells overexpressing human Cu/Zn-superoxide dismutase – implication for gene dosage effect in Down syndrome. *Cell* **52**, 259-267.

Fantus, I. G., Kadota, S., Deragon, G., Foster, B. and Posner, B. I. (1989). Pervanadate [peroxide(s) of vanadate] mimics insulin action in rat adipocytes via activation of the insulin receptor tyrosine kinase. *Biochemistry* **28**, 8864-8871.

Finkel, T. (2000). Redox-dependent signal transduction. *FEBS Lett.* **476**, 52-54.

Fisher, P. R., Merkl, R. and Gerisch, G. (1989). Quantitative analysis of cell motility and chemotaxis in Dictyostelium discoideum by using an image processing system and a novel chemotaxis chamber providing stationary chemical gradients. *J. Biol. Chem.* **108**, 973-984.

Floyd, R. A. and Hensley, K. (2000). Nitrone inhibition of age-associated oxidative damage. *Ann. New York Acad. Sci.* **899**, 222-237.

Gamou, S. and Shimizu, N. (1995). Hydrogen peroxide preferentially enhances the tyrosine phosphorylation of epidermal growth factor receptor. *FEBS Lett.* **357**, 161-164.

Gerst, J. E., Benezra, M., Schimmer, A. and Salomon, Y. (1989). Phorbol ester impairs melanotropin receptor function and stimulates growth of cultured M2R melanoma cells. *Eur. J. Pharmacol.* **172**, 29-39.

Gotoh, Y. and Cooper, J. A. (1998). Reactive oxygen species- and dimerization-induced activation of apoptosis signal-regulating kinase 1 in tumor necrosis factor-alpha signal transduction. *J. Biol. Chem.* **273**, 17477-17482.

Gross, S., Brandis, A., Chen, L., Rosenbach-Belkin, V., Roehrs, S., Scherz, A. and Salomon, Y. (1997). Protein-A-mediated targeting of bacteriochlorophyll-IgG to Staphylococcus aureus: a model for enhanced site-specific photocytotoxicity. *Photochem. Photobiol.* **66**, 872-878.

Gross, S., Gilead, A., Scherz, A., Neeman, M. and Salomon, Y. (2003). Monitoring photodynamic therapy of solid tumors online by BOLD-contrast MRI. *Nat. Med.* **9**, 1327-1331.

Guyton, K. Z., Liu, Y., Gorospe, M., Xu, Q. and Holbrook, N. J. (1996). Activation of mitogen-activated protein kinase by H_2O_2. Role in cell survival following oxidant injury. *J. Biol. Chem.* **271**, 4138-4142.

Halliwell, B. and Gutteridge, J. M. C. (1999). *Free Radicals in Biology and Medicine*. Oxford: Oxford University Press.

Hayes, G. R. and Lockwood, D. H. (1987). Role of insulin receptor phosphorylation in the insulinomimetic effects of hydrogen peroxide. *Proc. Natl. Acad. Sci. USA* **84**, 8115-8119.

Heffetz, D., Bushkin, I., Dror, R. and Zick, Y. (1990). The insulinomimetic agents H_2O_2 and vanadate stimulate protein tyrosine phosphorylation in intact cells. *J. Biol. Chem.* **265**, 2896-2902.

Ichijo, H., Nishida, E., Irie, K., ten Dijke, P., Saitoh, M., Moriguchi, T., Takagi, M., Matsumoto, K., Miyazono, K. and Gotoh, Y. (1997). Induction of apoptosis by ASK1, a mammalian MAPKKK that activates SAPK/JNK and p38 signaling pathways. *Science* **275**, 90-94.

Jaaro, H., Rubinfeld, H., Hanoch, T. and Seger, R. (1997). Nuclear translocation of mitogen-activated protein kinase kinase (MEK1) in response to mitogenic stimulation. *Proc. Natl. Acad. Sci. USA* **94**, 3742-3747.

Kamata, H. and Hirata, H. (1999). Redox regulation of cellular signalling. *Cell Signal* **11**, 1-14.

Kamata, H., Shibukawa, Y., Oka, S. I. and Hirata, H. (2000). Epidermal growth factor receptor is modulated by redox through multiple mechanisms. Effects of reductants and H_2O_2. *Eur. J. Biochem.* **267**, 1933-1944.

Kim, B. Y., Han, M. J. and Chung, A. S. (2001). Effects of reactive oxygen species on proliferation of Chinese hamster lung fibroblast (V79) cells. *Free Radic. Biol. Med.* **30**, 686-698.

Klotz, L. O., Pellieux, C., Briviba, K., Pierlot, C., Aubry, J. M. and Sies, H. (1999). Mitogen-activated protein kinase (p38-, JNK-, ERK-) activation pattern induced by extracellular and intracellular singlet oxygen and UVA. *Eur. J. Biochem.* **260**, 917-922.

Knebel, A., Rahmsdorf, H. J., Ullrich, A. and Herrlich, P. (1996). Dephosphorylation of receptor tyrosine kinases as target of regulation by radiation, oxidants or alkylating agents. *EMBO J.* **15**, 5314-5325.

Konan, Y. N., Gurny, R. and Allemann, E. (2002). State of the art in the delivery of photosensitizers for photodynamic therapy. *J. Photochem. Photobiol. B* **66**, 89-106.

Konishi, H., Matsuzaki, H., Tanaka, M., Takemura, Y., Kuroda, S., Ono, Y. and Kikkawa, U. (1997). Activation of protein kinase B (Akt/RAC-protein kinase) by cellular stress and its association with heat shock protein Hsp27. *FEBS Lett.* **410**, 493-498.

Konorev, E. A., Kennedy, M. C. and Kalyanaraman, B. (1999). Cell-permeable superoxide dismutase and glutathione peroxidase mimetics afford superior protection against doxorubicin-induced cardiotoxicity: the role of reactive oxygen and nitrogen intermediates. *Arch. Biochem. Biophys.* **368**, 421-428.

Koudinova, N. V., Pinthus, J. H., Brandis, A., Brenner, O., Bendel, P., Ramon, J., Eshhar, Z., Scherz, A. and Salomon, Y. (2003). Photodynamic therapy with Pd-Bacteriopheophorbide (TOOKAD): successful in vivo treatment of human prostatic small cell carcinoma xenografts. *Int. J. Cancer* **104**, 782-789.

Lander, H. M., Hajjar, D. P., Hempstead, B. L., Mirza, U. A., Chait, B. T., Campbell, S. and Quilliam, L. A. (1997). A molecular redox switch on p21(ras). Structural basis for the nitric oxide-p21(ras) interaction. *J. Biol. Chem.* **272**, 4323-4326.

LeBel, C. P., Ischiropoulos, H. and Bondy, S. C. (1992). Evaluation of the probe 2',7'-dichlorofluorescin as an indicator of reactive oxygen species formation and oxidative stress. *Chem. Res. Toxicol.* **5**, 227-231.

Lee, S. R., Kwon, K. S., Kim, S. R. and Rhee, S. G. (1998). Reversible inactivation of protein-tyrosine phosphatase 1B in A431 cells stimulated with epidermal growth factor. *J. Biol. Chem.* **273**, 15366-15372.

Lopez-Ongil, S., Senchak, V., Saura, M., Zaragoza, C., Ames, M., Ballermann, B., Rodriguez-Puyol, M., Rodriguez-Puyol, D. and

Lowenstein, C. J. (2000). Superoxide regulation of endothelin-converting enzyme. *J. Biol. Chem.* **275**, 26423-26427.

Meyer, M., Schreck, R. and Baeuerle, P. A. (1993). H_2O_2 and antioxidants have opposite effects on activation of NF-kappa B and AP-1 in intact cells: AP-1 as secondary antioxidant-responsive factor. *EMBO J.* **12**, 2005-2015.

Mori, K., Shibanuma, M. and Nose, K. (2004). Invasive potential induced under long-term oxidative stress in mammary epithelial cells. *Cancer Res.* **64**, 7464-7472.

Nemani, R. and Lee, E. Y. (1993). Reactivity of sulfhydryl groups of the catalytic subunits of rabbit skeletal muscle protein phosphatases 1 and 2A. *Arch. Biochem. Biophys.* **300**, 24-29.

Olszanecki, R., Kozlovski, V. I., Chlopicki, S. and Gryglewski, R. J. (2002). Paradoxical augmentation of bradykinin-induced vasodilatation by xanthine/xanthine oxidase-derived free radicals in isolated guinea pig heart. *J. Physiol. Pharmacol.* **53**, 689-699.

Plaks, V., Posen, Y., Mazor, O., Brandis, A., Scherz, A. and Salomon, Y. (2004). Homologous adaptation to oxidative stress induced by the photosensitized Pd-bacteriochlorophyll derivative (WST11) in cultured endothelial cells. *J. Biol. Chem.* **279**, 45713-45720.

Preise, D., Mazor, O., Koudinova, N., Liscovitch, M., Scherz, A. and Salomon, Y. (2003). Bypass of tumor drug resistance by antivascular therapy. *Neoplasia* **5**, 475-480.

Preston, T. J., Muller, W. J. and Singh, G. (2001). Scavenging of extracellular H_2O_2 by catalase inhibits the proliferation of HER-2/Neu-transformed rat-1 fibroblasts through the induction of a stress response. *J. Biol. Chem.* **276**, 9558-9564.

Remacle, J., Raes, M., Toussaint, O., Renard, P. and Rao, G. (1995). Low levels of reactive oxygen species as modulators of cell function. *Mutat. Res.* **316**, 103-122.

Robinson, K. A., Stewart, C. A., Pye, Q. N., Nguyen, X., Kenney, L., Salzman, S., Floyd, R. A. and Hensley, K. (1999). Redox-sensitive protein phosphatase activity regulates the phosphorylation state of p38 protein kinase in primary astrocyte culture. *J. Neurosci. Res.* **55**, 724-732.

Rosenkranz, A. A., Jans, D. A. and Sobolev, A. S. (2000). Targeted intracellular delivery of photosensitizers to enhance photodynamic efficiency. *Immunol. Cell Biol.* **78**, 452-464.

Saitoh, M., Nishitoh, H., Fujii, M., Takeda, K., Tobiume, K., Sawada, Y., Kawabata, M., Miyazono, K. and Ichijo, H. (1998). Mammalian thioredoxin is a direct inhibitor of apoptosis signal-regulating kinase (ASK) 1. *EMBO J.* **17**, 2596-2606.

Scherz, A., Fiedor, L., and Salomon, Y. (1997). Chlorophyll and bacteriochlorophyll derivatives, their preparation and pharmacological compositions comprising them. *US Patent 5,650,292.*

Scherz, A., Salomon, Y., Scheer, H., Hartwich, A. and Brandis, A. (2001). Synthetic metal substituted bacteriochlorophyll derivatives and the use thereof. *US Patent 6,333,319*.

Scherz, A., Salomon, Y., Brandis, A. and Scheer, H. (2003). Palladium-substituted bacteriochlorophyll derivatives and use thereof. *US Patent 6,569,846*.

Scherz, A., Salomon, Y. and Fiedor, L. (2000). Chlorophyll and bacteriochlorophyll derivatives, their preparation and pharmacological compositions comprising them. *European Patent 0,584,552*.

Schreiber, S., Gross, S., Brandis, A., Harmelin, A., Rosenbach-Belkin, V., Scherz, A. and Salomon, Y. (2002). Local photodynamic therapy (PDT) of rat C6 glioma xenografts with Pd-bacteriopheophorbide leads to decreased metastases and increase of animal cure compared with surgery. *Int. J. Cancer.* **99**, 279-285.

Suzuki, Y. J., Forman, H. J. and Sevanian, A. (1997). Oxidants as stimulators of signal transduction. *Free Radic. Biol. Med.* **22**, 269-285.

Tao, J. S. J., Pelech, S. L., Wong, G. and Levy, J. G. (1996). Stimulation of stress-activated protein kinase and p38 HOG1 kinase in murine keratinocytes following photodynamic therapy with benzoporphyrin derivative. *J. Biol. Chem.* **271**, 27107-27115.

Tas, J. and Westerneng, G. (1981). Fundamental aspects of the interaction of propidium diiodide with nuclei acids studied in a model system of polyacrylamide films. *J. Histochem. Cytochem.* **29**, 929-936.

Vakrat, Y., Weiner, L., Brandis, A., Mazor, O., Hami, R., Gross, S., Schreiber, S., Salomon, Y. and Scherz, A. (1999). Bacteriochlorophyll derivatives: Phototoxicity, hydrophobicity & oxygen radicals production. *J. Free Radic. Biol. Med.* **27 Suppl. 1**, S129 (abstract).

Vakrat-Haglili, Y., Weinner, L., Brumfeld, V., Brandis, A., Sarna, T., Pawlak, A., Rozanowska, M., Wrona, M., Wilson, B. C., McElroy, B. et al. (2002). Investigating the photophysical and photochemical mechanism of a novel sensitizer Pd- Bacteriopheophorbide by using ESR and spin trapping technique. *Proceedings of 7th International Symposium on Spin Trapping. July 7-11*, Chapel Hill, NC, USA.

Vakrat-Haglili, Y., Weiner, L., Brumfeld, V., Brandis, A., Salomon, Y., Macllroy, B., Wilson, B., Pawlak, A., Rozanowska, M., Sarna, T. and Scherz, A. (2005). The microenvironment effect on the generation of reactive oxygen species by Pd- Bactheriopheophorbide. *J. Am. Chem. Soc*. (in press).

Vazquez-Torres, A., Jones-Carson, J., Mastroeni, P., Ischiropoulos, H. and Fang, F. C. (2000). Antimicrobial actions of the NADPH phagocyte oxidase and inducible nitric oxide synthase in experimental salmonellosis. I. Effects on microbial killing by activated peritoneal macrophages in vitro. *J. Exp. Med.* **192**, 227-236.

Xue, L., He, J. and Oleinick, N. L. (1999). Promotion of photodynamic therapy-induced apoptosis by stress kinases. *Cell Death Differ.* **6**, 855-864.

Yung, Y., Yao, Z., Aebersold, D. M., Hanoch, T. and Seger, R. (2001). Altered regulation of ERK1b by MEK1 and PTP-SL and modified Elk1 phosphorylation by ERK1b are caused by abrogation of the regulatory C-terminal sequence of ERKs. *J. Biol. Chem.* **276**, 35280-35289.

Zhao, H., Kalivendi, S., Zhang, H., Joseph, J., Nithipatikom, K., Vasquez-Vivar, J. and Kalyanaraman, B. (2003). Superoxide reacts with hydroethidine but forms a fluorescent product that is distinctly different from ethidium: potential implications in intracellular fluorescence detection of superoxide. *Free Radic. Biol. Med.* **34**, 1359-1368.

Zilberstein, J., Schreiber, S., Bloemers, M. C., Bendel, P., Neeman, M., Schechtman, E., Kohen, F., Scherz, A. and Salomon, Y. (2001). Antivascular treatment of solid melanoma tumors with bacteriochlorophyll-serine-based photodynamic therapy. *Photochem. Photobiol.* **73**, 257-266.

Journal of Cell Science